JACC: CARDIOVASCULAR INTERVENTIONS
VOL. 9, NO. 19, 2016

ISSN 1936-8798/$36.00
PUBLISHED BY ELSEVIER
http://dx.doi.org/10.1016/j.jcin.2016.07.013

Diagnostic Accuracy of Fast Computational Approaches to Derive Fractional Flow Reserve From Diagnostic Coronary Angiography

The International Multicenter FAVOR Pilot Study

Shengxian Tu, PhD,[a] Jelmer Westra, MS,[b] Junqing Yang, MD,[c] Clemens von Birgelen, MD, PhD,[d] Angela Ferrara, MD,[e] Mariano Pellicano, MD,[e,f] Holger Nef, MD,[g] Matteo Tebaldi, MD,[h] Yoshinobu Murasato, MD, PhD,[i] Alexandra Lansky, MD, PhD,[j] Emanuele Barbato, MD, PhD,[e,f] Liefke C. van der Heijden, MD,[d] Johan H.C. Reiber, PhD,[k] Niels R. Holm, MD,[b] William Wijns, MD, PhD,[e,l] on behalf of the FAVOR Pilot Trial Study Group

ABSTRACT

OBJECTIVES The aim of this prospective multicenter study was to identify the optimal approach for simple and fast fractional flow reserve (FFR) computation from radiographic coronary angiography, called quantitative flow ratio (QFR).

BACKGROUND A novel, rapid computation of QFR pullbacks from 3-dimensional quantitative coronary angiography was developed recently.

METHODS QFR was derived from 3 flow models with: 1) fixed empiric hyperemic flow velocity (fixed-flow QFR [fQFR]); 2) modeled hyperemic flow velocity derived from angiography without drug-induced hyperemia (contrast-flow QFR [cQFR]); and 3) measured hyperemic flow velocity derived from angiography during adenosine-induced hyperemia (adenosine-flow QFR [aQFR]). Pressure wire-derived FFR, measured during maximal hyperemia, served as the reference. Separate independent core laboratories analyzed angiographic images and pressure tracings from 8 centers in 7 countries.

RESULTS The QFR and FFR from 84 vessels in 73 patients with intermediate coronary lesions were compared. Mean angiographic percent diameter stenosis (DS%) was 46.1 ± 8.9%; 27 vessels (32%) had FFR ≤ 0.80. Good agreement with FFR was observed for fQFR, cQFR, and aQFR, with mean differences of 0.003 ± 0.068 ($p = 0.66$), 0.001 ± 0.059 ($p = 0.90$), and −0.001 ± 0.065 ($p = 0.90$), respectively. The overall diagnostic accuracy for identifying an FFR of ≤0.80 was 80% (95% confidence interval [CI]: 71% to 89%), 86% (95% CI: 78% to 93%), and 87% (95% CI: 80% to 94%). The area under the receiver-operating characteristic curve was higher for cQFR than fQFR (difference: 0.04; 95% CI: 0.01 to 0.08; $p < 0.01$), but did not differ significantly between cQFR and aQFR (difference: 0.01; 95% CI: -0.04 to 0.06; $p = 0.65$). Compared with DS%, both cQFR and aQFR increased the area under the receiver-operating characteristic curve by 0.20 ($p < 0.01$) and 0.19 ($p < 0.01$). The positive likelihood ratio was 4.8, 8.4, and 8.9 for fQFR, cQFR, and aQFR, with negative likelihood ratio of 0.4, 0.3, and 0.2, respectively.

CONCLUSIONS The QFR computation improved the diagnostic accuracy of 3-dimensional quantitative coronary angiography-based identification of stenosis significance. The favorable results of cQFR that does not require pharmacologic hyperemia induction bears the potential of a wider adoption of FFR-based lesion assessment through a reduction in procedure time, risk, and costs. (J Am Coll Cardiol Intv 2016;9:2024–35) © 2016 by the American College of Cardiology Foundation.

Diagnostic coronary angiography is the established standard for identification of coronary artery disease. However, angiographic images frequently fail to describe the functional significance of a stenosis, which can lead to unnecessary revascularizations or deferral of necessary interventions (1,2). Fractional flow reserve (FFR) is a precise index that reveals the specific ischemic potential of coronary obstructions. Numerous studies have documented favorable clinical outcomes for FFR-guided coronary interventions in patients with stable coronary artery disease (3–7).

SEE PAGE 2036

Despite the clear advantages, the clinical adoption of FFR has been variable and slow (8). A survey reported in 2014 showed that of 495 interventional cardiologists evaluating the same 12 intermediate stenoses, 27% would not apply FFR at all, despite the fact that all cases met the European Society of Cardiology Class I recommendations for FFR measurement (9). A tool that allows calculating FFR without the use of costly pressure wires and the administration of adenosine could increase the adoption of FFR.

With recent advances in computational sciences, computational fluid dynamics has been applied to noninvasive imaging modalities such as multislice computed tomography for the computation of FFR, showing good diagnostic performances (10,11). Invasive quantitative coronary angiography (QCA)-based computational FFR by various methods was also reported with promising results (12–14). Despite promising initial results, FFR computation is still to be improved to increase the feasibility for use in routine clinical practice.

A novel approach enabling rapid computation of FFR pullbacks from 3-dimensional quantitative coronary angiography (3D QCA) was recently developed (15). The computational FFR, denoted as quantitative flow ratio (QFR), can be obtained using 3 different flow models: 1) a fixed empiric hyperemic flow velocity (HFV), derived from previous FFR studies (12) (fixed-flow QFR [fQFR]); 2) modelled HFV derived from coronary angiography without pharmacologically induced hyperemia (contrast-flow QFR [cQFR]), that is, the contrast flow was converted into the virtual hyperemic flow based on data derived from previous studies (12), and cQFR was computed as if adenosine was actually used; and 3) measured HFV derived from coronary angiography during adenosine-induced maximum hyperemia (adenosine-flow QFR [aQFR]). It is unknown which of these computational models is most precise. Therefore, we performed a prospective multicenter study to compare the diagnostic performance of these QFR computational models as compared with pressure wire-derived FFR.

ABBREVIATIONS AND ACRONYMS

aQFR = adenosine-flow quantitative flow ratio

AUC = area under the receiver-operating characteristic curve

CI = confidence interval

cQFR = contrast-flow quantitative flow ratio

DS% = percent diameter stenosis

FFR = fractional flow reserve

fQFR = fixed-flow quantitative flow ratio

HFV = hyperemic flow velocity

QCA = quantitative coronary angiography

QFR = quantitative flow ratio

METHODS

STUDY DESIGN. The prospective, observational, multicenter FAVOR (Functional Assessment by

From the [a]Biomedical Instrument Institute, School of Biomedical Engineering, Shanghai Jiao Tong University, Shanghai, China; [b]Department of Cardiology, Aarhus University Hospital, Skejby, Denmark; [c]Department of Cardiology, Guangdong General Hospital, Guangzhou, China; [d]Department of Cardiology, Thoraxcentrum Twente, Medisch Spectrum Twente, and Health Technology and Services Research, MIRA Institute, University of Twente, Enschede, the Netherlands; [e]Cardiovascular Research Centre, OLV Hospital, Aalst, Belgium; [f]Department of Advanced Biomedical Sciences, University of Naples, Federico II, Naples, Italy; [g]Department of Cardiology and Angiology, University of Giessen, Giessen, Germany; [h]Cardiovascular Institute, Azienda Ospedaliero-Universitaria di Ferrara, Ferrara, Italy; [i]Department of Cardiology, Clinical Research Center, Kyushu Medical Center, Fukuoka, Japan; [j]Section of Cardiovascular Medicine, Yale University School of Medicine, New Haven, Connecticut; [k]Department of Radiology, Leiden University Medical Center, Leiden, the Netherlands; and [l]The Lambe Institute for Translational Medicine and Curam, National University of Ireland, Galway, and Saolta University Healthcare Group, Galway, Ireland. Dr. Tu has received a research grant from Medis Medical Imaging Systems BV. Dr. von Birgelen has been a consultant to Boston Scientific and Medtronic; received lecture fees from AstraZeneca; and his institution has received research grants from AstraZeneca, Biotronik, Boston Scientific, and Medtronic. Dr. Reiber is the CEO of Medis; and has a part-time appointment at Leiden University Medical Center as Prof. of Medical Imaging. Dr. Holm has received speaker fees from St. Jude Medical, Biotronik, and Terumo; and institutional research grants from St. Jude Medical, Terumo, Boston Scientific, Medtronic Biotronic, Medis medical imaging, and Cordis. Cardiovascular Research Center Aalst receives institutional grant support and consultancy fees on behalf of Drs. Wijns and Barbato from St. Jude Medical, and other device and pharmaceutical companies. Expenses associated with study enrollment and procedures are covered by the participating centers. The 3D angiographic reconstruction and computation of FFR at ClinFact, the Netherlands, and the FFR core lab readings at Aarhus University, Denmark, are performed at their own expenses. In addition, Shanghai Jiao Tong University received a research grant on behalf of Dr. Tu from Medis Medical Imaging Systems and 2 research grants from the Natural Science Foundation of China (Grant Number 31500797 and 81570456) that supported the development of the methods for coronary angiographic reconstruction and computation of FFR. All other authors have reported that they have no relationships relevant to the contents of this paper to disclose. This is an investigator-initiated study.

Manuscript received April 22, 2016; revised manuscript received June 25, 2016, accepted June 30, 2016.

Various Flow Reconstructions) pilot study investigated offline computation of QFR as compared with conventional pressure wire-based FFR as the standard reference. The study was conducted at 8 sites in 7 countries on 3 continents: Europe (Belgium, Italy [n = 2], the Netherlands, Germany), Asia (China, Japan), and North America (the United States). Participating centers are listed in Online Appendix I. The study complied with the Declaration of Helsinki for investigation in human beings. The study protocol was approved by the institutional review boards of the individual centers and—as appropriate—by local and/or national medical ethical committees. All patients provided written informed consent before study enrolment.

STUDY POPULATION. Patients ≥18 years of age with stable angina pectoris and indication for invasive coronary angiography and FFR assessment were included if able to provide written informed consent. Exclusion criteria were contraindications to adenosine or adenosine triphosphate administration. Angiographic inclusion criteria were: 1) ≥1 lesion with 30% to 80% diameter stenosis (DS%) by visual estimation; and 2) FFR measurement deemed feasible by the operator. Exclusion criteria were: 1) ostial left main or ostial right coronary artery lesion; and 2) prior coronary artery bypass grafting of the interrogated vessels.

STUDY PROCEDURE. Invasive coronary angiography was performed according to best local practice. If FFR measurement was indicated, the stenosis was assessed by pressure wire using the following strategies (**Figure 1**): 1) pressure wire baseline distal coronary pressure to aortic pressure ratio; then 2) FFR by intravenous adenosine/adenosine triphosphate infusion. Two angiographic projections were acquired during each measurement. Subsequent clinical decision making was based on clinical guidelines, at the operator's discretion, and was not study related. Detailed study procedures are described in Online Appendix II.

COMPUTATION OF QFR. Computation of QFR was performed offline, using a prototype software package (QAngio XA 3D prototype, Medis Medical Imaging System, Leiden, the Netherlands). In the first step, 2 diagnostic angiographic projections, at least 25° apart, were selected and 3D reconstruction of the interrogated vessel without its side branches was performed, as previously described (16) and 3D QCA data were readily available. Then, the software computed within a minute the following 3 QFR pullbacks, based on a recently published method (15). The QFR computation was based on the underlying principles: 1) coronary pressure remains constant through normal epicardial coronary arteries (17); 2) the amount of pressure drop is determined by the stenosis geometry and the flow moving through the stenosis, described by the fluid dynamic equations (18); 3) the stenosis geometry can be characterized by the deviation of the diseased lumen sizing with respect to the reference sizing, i.e., the healthy lumen as if there was no stenosis, by 3D QCA (12); and 4) Coronary flow velocity is preserved distally relative to proximal flow velocity (19), and the mass flow rate in the main coronary arteries decreases with the tapering of the arteries due to the presence of side branches. Hence, the mass flow rate at each location along the interrogated vessel can be determined by the mean flow velocity and the reference sizing from 3D QCA. Details of the computational methods are described in Online Appendix II.

The following 3 QFR computations were performed, based on the different mean hyperemic flow velocities:

1. The fQFR pullback: a fixed empiric HFV of 0.35 m/s that was derived from previous FFR studies (12) was used for computation, and then a comparison with the pressure wire-based FFR was performed.
2. The cQFR pullback: frame count analysis was performed separately on the 2 diagnostic angiographic projections without pharmacologically induced hyperemia, and the modelled HFVs were derived by which the software computed 2 new QFR pullbacks. The analyst chose the QFR pullback based on best image quality (most well-defined contrast-flow) in the frame count analysis as the cQFR pullback to compare with the pressure wire-based FFR.

   The following quadratic function was applied to quantify the relation between the baseline flow velocity with injection of contrast medium (contrast-flow velocity, CFV) and the HFV:

   $$HFV = a0 + a1 \cdot CFV + a2 \cdot CFV^2$$

   Where a0, a1, and a2 are parameters that characterize the best fitting curve that minimized the mean distance from all sample points in the training datasets to the fitting curve. The datasets from a previous study (12) were used as the training datasets and the optimal values were obtained at a0 = 0.10; a1 = 1.55 and a2 = -0.93, with an R^2 of 0.34.
3. The aQFR pullback: frame count analysis was performed separately on the 2 angiographic projections that were acquired during hyperemia,

FIGURE 1 Schematic Presentation of Study Procedures Showing the 2 Main Acquisition Steps

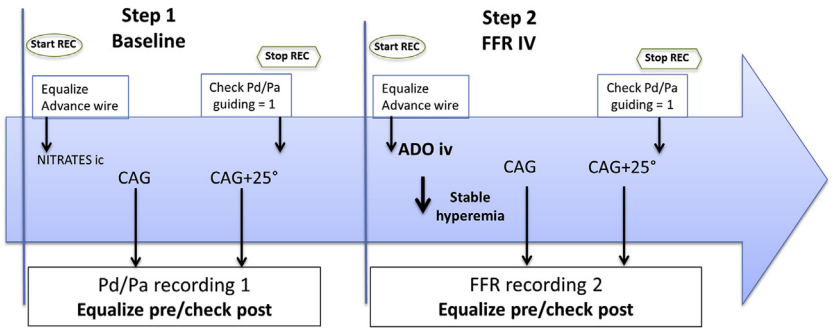

First, the assessment of nonhyperemia distal coronary pressure to aortic pressure ratio and the corresponding angiographic runs for computation of fQFR and cQFR. Second, assessment of FFR and acquisition of angiographic runs during intravenous adenosine infusion for computation of aQFR. aQFR = adenosine-flow QFR; cQFR = contrast-flow QFR; FFR = fractional flow reserve; fQFR = fixed-flow QFR; QFR = quantitative flow ratio.

induced by intravenous administration of adenosine or adenosine triphosphate. The "real" HFVs were derived and the software calculated 2 new QFR pullbacks. The analyst chose the QFR pullback based on best image quality in the frame count analysis as the aQFR pullback to compare with the pressure wire-based FFR.

The QFR value at the position that matched the location of the pressure transducer on the pressure wire was used for comparison with the FFR value measured by the pressure wire.

Of note, the flow velocity was derived by dividing the arterial segment length from 3D QCA and the corresponding dye flow time from frame count analysis. The software allowed for selection of a subsegment of the reconstructed artery with good visualization of the dye flow for calculation of flow velocity.

DATA MANAGEMENT AND ANALYSIS. Source data were collected on-line using dedicated worksheets. Detailed case report forms were completed with supplemental data for each patient. The source data were maintained by each participating center. Study angiograms and FFR traces were anonymized and submitted to 2 separate, independent, dedicated core laboratories: ClinFact (Leiden, the Netherlands) and Interventional Coronary Imaging Core Laboratory (Aarhus University Hospital, Aarhus, Denmark). Study personnel responsible for QFR computation were not present in the catheter laboratory during the procedure and were blinded to the results of the pressure wire-based FFR analysis and vice versa.

THE REFERENCE STANDARD OF FUNCTIONAL SIGNIFICANCE. Pressure wire-derived FFR measured during maximal stable hyperemia, induced by intravenous adenosine/adenosine triphosphate infusion (core laboratory reading), is used as the reference standard from which the diagnostic accuracy of QFR was derived.

STATISTICS. Descriptive statistics are reported as mean ± SD, median (interquartile range [IQR]), or frequencies (%), as appropriate. Data were analyzed on a per-patient basis for clinical characteristics and on a per-vessel basis for the remaining calculations. Normal distribution was tested with the Shapiro-Wilk test. Correlation between QFR and FFR was determined by Pearson's correlation coefficient (r). Pairwise comparisons were made with Student t test or Mann-Whitney U tests, as appropriate. Sensitivity, specificity, positive predictive value, negative predictive value, positive likelihood ratio, negative likelihood ratio, and diagnostic accuracy were defined from the calculated receiver operator characteristic curves. The 95% confidence interval (CI) was added, as appropriate. Receiver operator characteristic curves were compared using the DeLong method. Analysis of receiver operator characteristic curves was performed by MedCalc version 13.0 (Mariakerke, Belgium). Other statistical analyses were performed with IBM SPSS version 22.0 (SPSS Inc., Chicago, Illinois). A 2-sided p value of <0.05 was considered significant. The area under the receiver-operating characteristic curve (AUC) and standard error were determined for the individual study centers. Heterogeneity between the study centers was assessed using the I^2 statistic (20); we assumed heterogeneity when the degree of inconsistency (using I^2 statistics) was >50% with an associated p value of <0.05.

FIGURE 2 Study Flow Chart

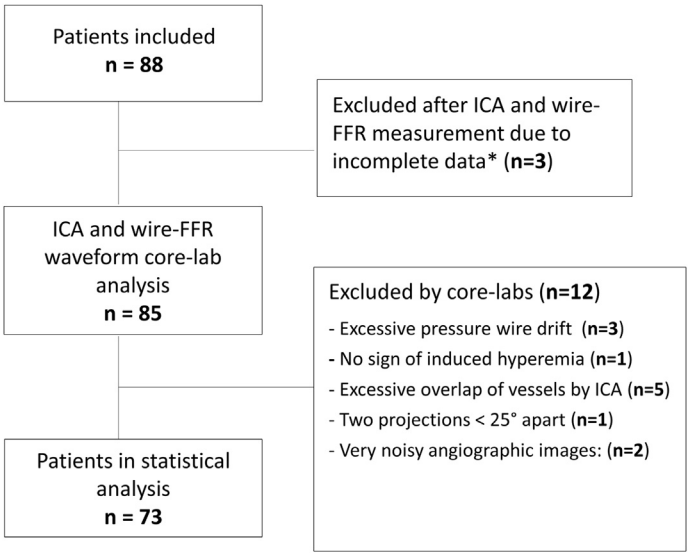

*Pressure wire-based FFR traces were missing for the cases that were not analyzed by the ICA/FFR core laboratories. ICA = invasive coronary angiography; other abbreviation as in Figure 1.

RESULTS

BASELINE CLINICAL AND LESION CHARACTERISTICS. A total of 88 patients with intermediate coronary stenoses were included from December 17, 2014, to September 29, 2015 (enrollment at different sites was not simultaneous based on different regulatory approval timelines). Fifteen patients (16 vessels) were excluded due to pre-defined criteria (Figure 2 provides reasons for their exclusion). This resulted in 84 vessels (1 left main stem, 46 left anterior descending arteries, 1 diagonal branch, 12 left circumflex arteries, 5 obtuse marginal branches, and 19 right coronary arteries) from 73 patients that were included in the current analysis. The clinical characteristics of these patients are listed in Table 1, and Table 2 shows the lesion characteristics. The interrogated vessels had a minimum lumen diameter of 1.52 ± 0.36 mm, a DS% of 46.1 ± 8.9%, a percent area stenosis of 64.5 ± 10.9%, and a pressure-derived FFR of 0.84 ± 0.08 (median 0.85; IQR: 0.77 to 0.89). An FFR of ≤0.80 was measured in 27 vessels (32.1%).

TABLE 1 Baseline Patient Characteristics (n = 73)

Age, yrs	65.8 ± 8.9
Male	61 (83.5)
Body mass index, kg/m^2	26.3 ± 6.3
Hypertension	32 (43.8)
Diabetes mellitus	17 (27.4)*
Cardiovascular history	
Prior myocardial infarction	23 (31.5)
Prior PCI	28 (38.4)
Prior CABG	2 (2.7)

Values are mean ± SD or n (%). *Data missing in 11 patients.
CABG = coronary artery bypass surgery; IQR = interquartile range; PCI = percutaneous coronary intervention.

CORRELATION AND AGREEMENT BETWEEN QFR AND FFR. The mean pressure at the tip of the guiding catheter was 95 ± 14 mm Hg during coronary angiography without hyperemia and 88 ± 18 mm Hg during maximum pharmacologically induced hyperemia. The mean measured flow velocity was 0.20m/s (median 0.19 m/s; IQR: 0.15 to 0.24 m/s; range 0.09 to 0.55 m/s) after injection of contrast medium before induced hyperemia and the corresponding cQFR was 0.84 (median 0.85; IQR: 0.79 to 0.90). The mean flow velocity increased to 0.37 m/s (median 0.37 m/s; IQR: 0.28 to 0.43 m/s; range 0.17 to 0.78 m/s) during maximum hyperemia and the corresponding aQFR was 0.84 (median 0.84; IQR: 0.79 to 0.91). Representative examples of computation of QFR using different flow models are shown in Figures 3 and 4. Good correlations with standard FFR were observed for fQFR, cQFR, and aQFR ($r = 0.69$ [$p < 0.001$]; $r = 0.77$ [$p < 0.001$]; $r = 0.72$ [$p < 0.001$], respectively) (Figure 5). There was also good agreement between measured FFR and QFR computed by these 3 flow models (mean differences: 0.003 ± 0.068 [$p = 0.66$]; 0.001 ± 0.059 [$p = 0.90$]; and -0.001 ± 0.065 [$p = 0.89$], respectively).

ACCURACY OF QFR FOR DIAGNOSIS OF FUNCTIONALLY SIGNIFICANT STENOSES. Using a cutoff value of ≤0.80 for QFR, a higher AUC in per-vessel analysis was observed for fQFR (0.88; 95% CI: 0.79 to 0.94), cQFR (0.92; 95% CI: 0.85 to 0.97), and aQFR (0.91; 95% CI: 0.83 to 0.96), compared with a cutoff value of >50% for DS% by 3D QCA (0.72; 95% CI: 0.62 to 0.82) (Figure 6). The increase in AUC was 0.16 (95% CI: 0.05 to 0.26; $p < 0.01$), 0.20 (95% CI: 0.10 to 0.30; $p < 0.01$), and 0.19 (95% CI: 0.08 to 0.30; $p < 0.01$), for fQFR, cQFR, and aQFR, respectively. The AUC was significantly higher for cQFR compared with fQFR (difference: 0.04; 95% CI: 0.01 to 0.08; $p < 0.01$), while there was no difference in AUC for cQFR and aQFR (difference: 0.01; 95% CI: -0.04 to 0.06; $p = 0.65$). The overall diagnostic accuracy for identifying an FFR of ≤0.80 in per-vessel analysis was numerically the highest by aQFR (87%; 95% CI: 80% to 94%), followed by cQFR (86%; 95% CI: 78% to 93%) and

TABLE 2 Baseline Vessel and Procedural Characteristics (n = 84)

Lesion location	
Left main stem	1 (1.2)
Left anterior descending artery	46 (54.8)
Diagonal branch	1 (1.2)
Left circumflex artery	12 (14.3)
Obtuse marginal branch	5 (6.0)
Right coronary artery	19 (22.6)
Fractional flow reserve	
Mean ± SD	0.84 ± 0.08
Median [IQR]	0.85 [0.77–0.89]
Minimum lumen area, mm^2	1.94 [1.41–2.62]
Percent area stenosis, %	64.5 ± 4.5
Reference diameter, mm	2.84 [2.57–3.06]
Diffuse or serial lesions	30 (35.7)

Values are n (%), mean ± SD, or median [IQR].

fQFR (80%; 95% CI: 71% to 89%). Computation of QFR by diagnostic angiography without induced hyperemia (i.e., cQFR) substantially improved the diagnostic performance of coronary angiography, with a sensitivity of 74%, specificity of 91%, positive predictive value of 80%, negative predictive value of 88%, positive likelihood ratio of 8.4, and negative likelihood ratio of 0.3 (Table 3). Of note, when cQFR was >0.90 or ≤0.70, all stenoses were classified correctly as compared with standard pressure wire-derived FFR with the cutoff value of 0.80. When cQFR was >0.85 or ≤0.75, 50 out of 54 stenoses were correctly classified, as compared with the standard FFR measurement.

FEASIBILITY AND REPRODUCIBILITY OF QFR. The I^2 for the fQFR, cQFR, and aQFR was 0.00, indicating that the between-center variance component is small enough to be ignored. Sufficient quality for applying frame count in both angiographic projections was achieved in 79 vessels (94%) in the cQFR computation; in 5 vessels (6%) due to poor visualization of dye flow, frame count analysis was performed in 1 projection only. No statistically significant difference between cQFR computations based on frame count analysis on the 2 angiographic projections was found (difference: 0.003 ± 0.030; p = 0.31). In 73 vessels (87%), the angiographic quality during maximum hyperemia was sufficient for the computation of aQFR based on both angiographic projections, whereas in 11 vessels (13%) the frame count analysis could only be performed in 1 angiographic projection. No statistically significant difference between aQFR computations based on frame count analysis on the 2 hyperemic angiographic projections was found (difference: 0.005 ± 0.026; p = 0.12).

DISCUSSION

We have developed a novel approach that allows rapid *computation* of FFR during diagnostic coronary angiography. In the study population of 73 patients with intermediate coronary lesions in 84 vessels, the QFR showed good agreement with the pressure wire-determined standard FFR measurements. The agreement was particularly favorable with QFR derived from contrast-flow (cQFR) and adenosine-flow models (aQFR), which both incorporated patient-specific flow by frame count analysis. Positive and negative likelihood ratios were of diagnostic value for use in the individual patient with cQFR and aQFR, although the positive likelihood ratio was of insufficient diagnostic value to be clinically useful with fQFR and a DS% of ≥50% (21).

In this study, the vessel-based diagnostic accuracy for determining the functional significance of an intermediate stenosis (i.e., FFR ≤ 0.80) was only 65%, if based on a single 3D QCA anatomic parameter of diameter stenosis of ≥50%. This is in line with a recent study with online QCA, including 4,086 consecutive coronary stenoses with FFR measurements (22), and 2 studies with 3D QCA that showed similar results for the diagnostic accuracy of intermediate coronary lesions, regardless of the presence of bifurcation lesions (2,12). This implies that our study population reflects patients who are examined with FFR in routine clinical practice, where FFR is mostly used to evaluate intermediate coronary lesions. Notably, the inclusion of severely stenotic or only mildly obstructed vessel segments would have resulted in higher accuracy of DS% and QFR, albeit not representative of clinical practice. We found that applying QFR computation on top of 3D QCA on such a patient population significantly improved the diagnostic accuracy in identifying functionally significant coronary lesions. The diagnostic accuracy of all 3 QFR approaches for predicting an FFR of ≤0.80 was relatively high, ranging from 80% for QFR by the fixed-flow model (fQFR), to 86% and 87% for QFR derived from contrast-flow (cQFR) and adenosine-flow based (aQFR) models. Even use of the most straightforward model, which uses a fixed flow velocity for QFR computation, increased the AUC by 0.16. Of note, no additional user interaction is required to derive QFR from the fixed-flow model and the QFR computation is immediately available after the 3D QCA analysis. Nevertheless, the diagnostic accuracy of this simplified QFR computation is suboptimal. A positive likelihood ratio of 4.8 for fQFR implies that this approach is not of sufficient diagnostic value to be clinically useful (21).

FIGURE 3 Computation of QFR by Coronary Angiography on LAD With Physiologically Nonsignificant Stenoses

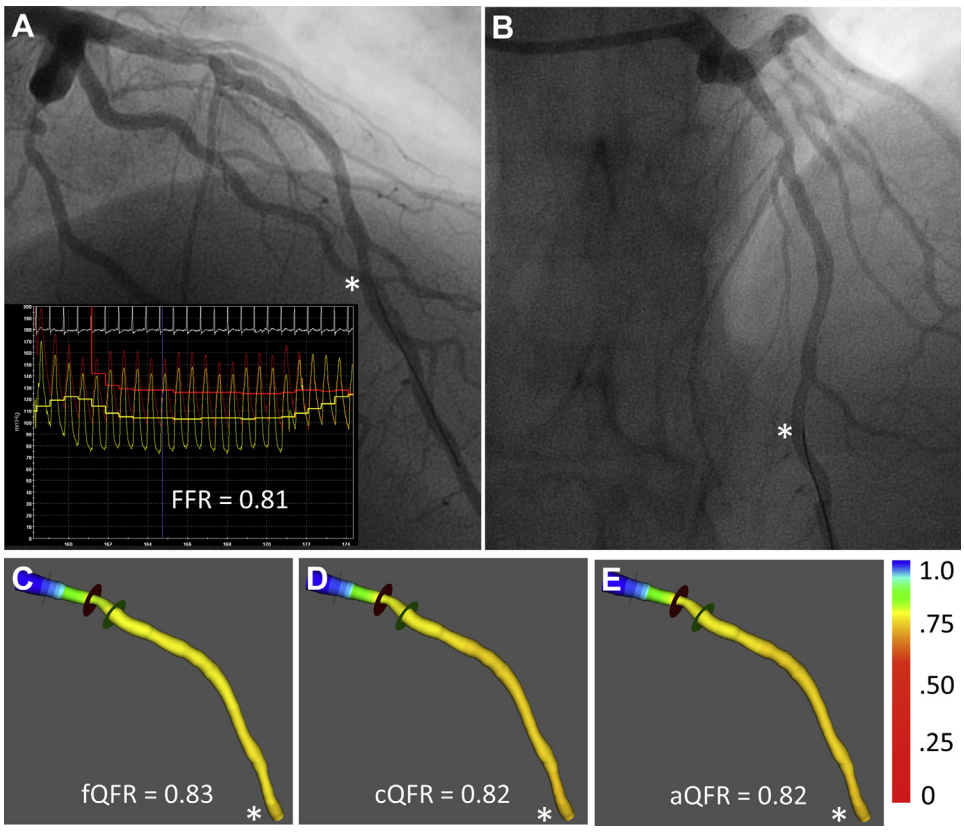

(A, B) Coronary angiography shows LAD with serial stenoses. The FFR measured by pressure wire at * was 0.81. **(C)** The computed fixed-flow QFR at * was 0.83. **(D)** The computed contrast-flow QFR was 0.82, and the mean flow velocity calculated on angiographic runs acquired without maximum hyperemia was 0.21 m/s. The modelled hyperemic flow velocity was 0.39 m/s. **(E)** The computed adenosine-flow QFR at * was 0.82, and the hyperemic flow velocity calculated on angiographic runs acquired during maximum hyperemia was 0.39 m/s. LAD = left descending artery; other abbreviations as in Figure 1.

In contrast, the transport time of the contrast medium can be used for a patient-specific estimation of coronary flow, which might improve FFR computation, as previously shown (12). Still, the user interaction required to identify the frames that correspond with the time for transporting the contrast medium through the interrogated vessel might introduce some bias and interobserver variation. Our study shows that the QFR computation based on a patient-specific contrast-flow model, derived from coronary angiography without pharmacologic hyperemia induction, improved the diagnostic accuracy as compared with the fixed-flow approach. However, QFR based on adenosine-induced hyperemia unexpectedly did not further improve the FFR estimation, compared with the contrast-flow–based model.

Several reasons might explain this observation. First, prior intracoronary injections of contrast medium induce submaximal hyperemia (23,24), which might have improved the correlation of QFR based on the contrast-flow and the adenosine-based hyperemic flow model. Leone et al. (24) observed a strong correlation between the contrast medium induced distal coronary pressure to aortic pressure ratio with respect to the FFR, indicating that the hyperemic flow can be modelled quite well by the contrast-flow. In our study, we systematically injected contrast medium with a forceful hand injection and followed a pre-defined protocol for invasive coronary angiography as specified in Online Appendix II, potentially improving the correlation between contrast-flow velocity and HFV. Hyperemia can also result from flow increases that follow replacement of blood by contrast (reactive hyperemia). Contrast injection can actually be used to measure FFR and results in submaximal hyperemia,

FIGURE 4 Computation of QFR by Coronary Angiography on RCA With Physiologically Significant Stenoses

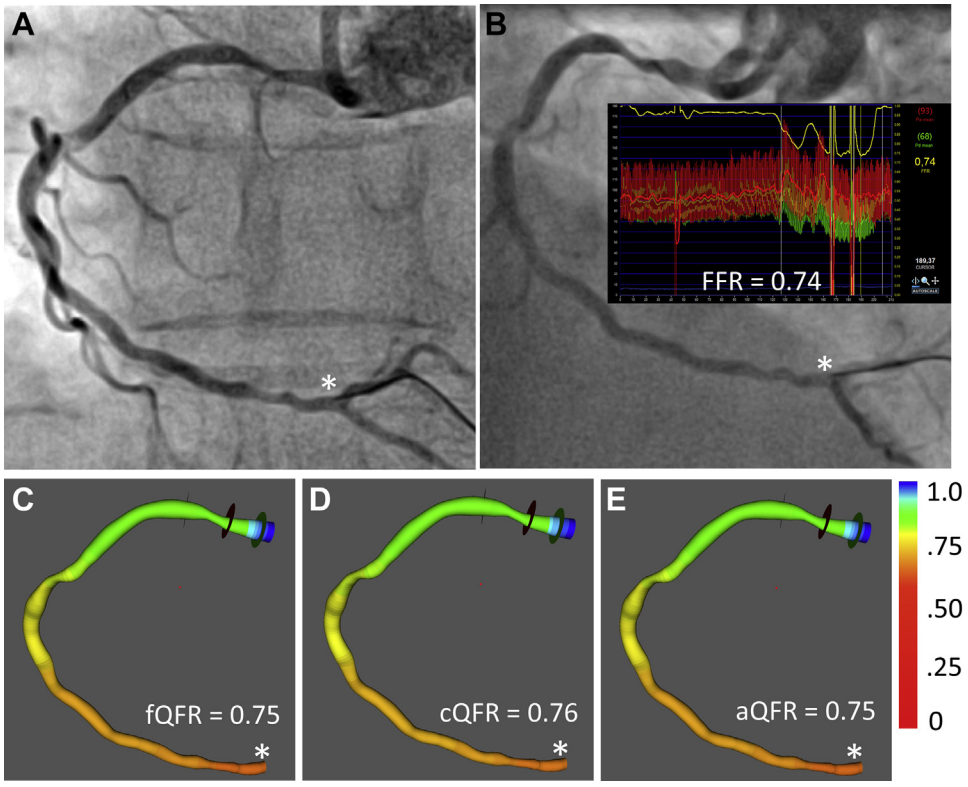

(A, B) Coronary angiography shows RCA with serial stenoses. The FFR measured by pressure wire at * was 0.74. **(C)** The computed fixed-flow QFR at * was 0.75. **(D)** The computed contrast-flow QFR was 0.76, and the mean flow velocity calculated on angiographic runs acquired without maximum hyperemia was 0.17 m/s. The modelled hyperemic flow velocity was 0.34 m/s. **(E)** The computed adenosine-flow QFR at * was 0.75, and the hyperemic flow velocity calculated on angiographic runs acquired during maximum hyperemia was 0.37 m/s. RCA = right coronary artery; other abbreviations as in **Figure 1**.

at 80% of adenosine flow on average (22). Of note, good correlation and agreement between cQFR and aQFR was observed (Online Appendix III). Second, the phase of the cardiac circle (i.e., systole versus diastole), during which the main passage of dye through the coronary vessel occurs, may affect coronary flow velocity. This is particularly relevant, if coronary flow velocity is very rapid, as for instance during pharmacologically induced maximum hyperemia (flow velocity is then almost doubled). In other words, if contrast medium passes through epicardial coronary vessels predominantly during systole, this may lead to an underestimation of mean flow velocity. The opposite may be true for predominantly diastolic passages of dye. Third, the use of adenosine for the induction of hyperemia increases both heartbeat and flow rate, which leads to a deterioration in angiographic image quality. In the current study, image quality was indeed more often inadequate for frame count analysis on both angiographic projections in the setting of QFR computation based on the adenosine-flow model than with the contrast-flow model (13% vs. 6%).

Compared with existing FFR computational methods based on computational fluid dynamics (12–14,25), our novel QFR computation approach is simple and very fast, which might greatly facilitate its potential integration in future routine clinical practice. A factor that contributes especially to the simplicity of the current approach is the fact that the reference diameter function from 3D QCA is used to compensate for the decrease in mass flow rate in the main vessel as side branches are taking off. In other words, our approach assumes that mean flow velocity will remain constant when crossing bifurcations, whereas the mass flow rate will decrease as side branches are taking off, which is reflected in tapering of the reference diameter function by 3D QCA. This

FIGURE 5 Correlation and Agreement Between FFR and QFR by the 3 Different Flow Models

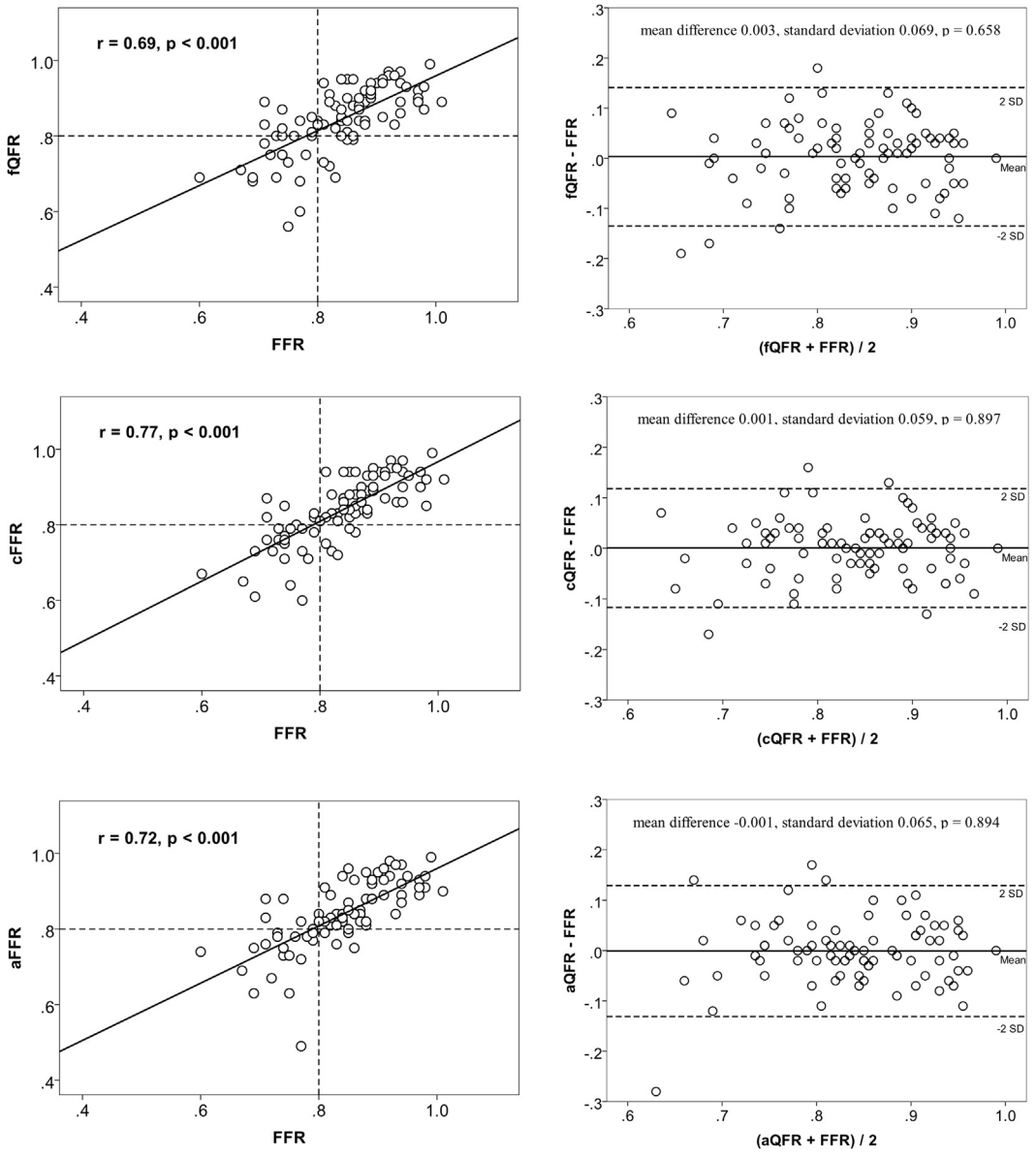

Good correlations **(left)** and agreements **(right)** were observed for all QFR computations with respect to conventional pressure wire-derived FFR. Abbreviations as in Figure 1.

assumption allows a more accurate computation of pressure decrease by assessing only the main vessel of interest (without reconstructing its side branches). In contrast, other conventional computational fluid dynamics approaches need to follow the principles of conservation of mass and momentum; therefore, neglecting side branches in angiographic reconstruction would lead to a substantial overestimation of coronary blood flow and pressure decrease in the vessel of interest (26). Despite the simplicity of the proposed QFR computational approach, we acknowledge that the use of reference diameter based on automatic contour detection may require extra user interaction when assessing diffuse coronary disease. However, a standard operation procedure that has been applied for QCA analysis (25) can be used to optimize the workflow. The QCA standard operation procedure

FIGURE 6 Comparison of Receiver Operating Curves for the Discrimination of Functionally Significant Stenoses

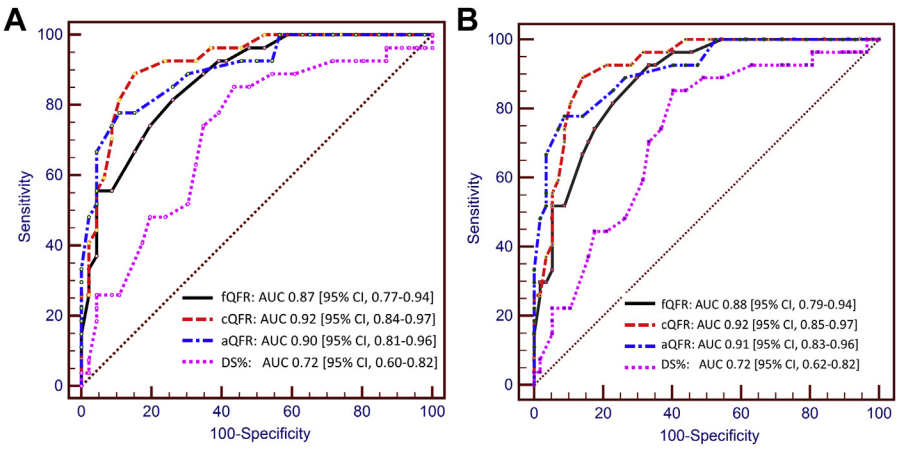

(A) Per patient. **(B)** Per vessel. The AUC was significantly higher for fQFR, cQFR, and aQFR, as compared with the anatomic parameter DS%. AUC = areas under the receiver-operator characteristics curve; DS% = percent diameter stenosis; other abbreviations as in Figure 1.

requires the user to "flag" out the diseased subsegments in the calculation of reference diameter function. This is particularly relevant in the case of diffuse disease, so that a reasonable estimation of the normal size of the vessel is obtained. Our validation studies (27) demonstrated the validity of this standard process, and the resulting low variability outcomes. In addition, the assumption of constant flow velocity might not be accurate in situations where flow distribution at coronary bifurcations has been altered, due to the presence of severe epicardial stenoses or regional microcirculatory dysfunction. This factor should impact less on the computation of cQFR than aQFR, because resting flow will be restricted only by very tight epicardial stenoses (28).

TABLE 3 Diagnostic Performance of QFR

	fQFR ≤0.8	cQFR ≤0.8	aQFR ≤0.8	%DS ≥50%
Per patient				
Accuracy	78 (68-88)	85 (77-93)	85 (77-93)	63 (52-74)
Sensitivity	67 (46-84)	74 (54-89)	78 (58-91)	48 (29-68)
Specificity	85 (71-94)	91 (79-98)	89 (76-96)	76 (61-87)
PPV	72 (51-88)	83 (63-95)	80 (64-91)	54 (33-74)
NPV	81 (67-91)	86 (73-94)	88 (71-97)	71 (57-83)
(+)LR	4.4 (2.1-9.1)	8.5 (3.3-22.3)	7.2 (3.1-16.8)	2.0 (1.1-3.8)
(-)LR	0.4 (0.2-0.7)	0.3 (0.1-0.5)	0.3 (0.1-0.5)	0.7 (0.5-1.0)
AUC	0.87 (0.77-0.94)	0.92 (0.84-0.97)	0.90 (0.81-0.96)	0.72 (0.60-0.82)
Per vessel				
Accuracy	80 (71-89)	86 (78-93)	87 (80-94)	65 (55-76)
Sensitivity	67 (46-84)	74 (54-89)	78 (58-91)	44 (26-65)
Specificity	86 (74-94)	91 (81-97)	91 (81-97)	79 (66-89)
PPV	69 (48-86)	80 (59-93)	81 (61-93)	50 (29-71)
NPV	85 (73-93)	88 (77-95)	90 (79-96)	75 (62-85)
(+)LR	4.8 (2.4-9.5)	8.4 (3.6-20.1)	8.9 (3.7-21.0)	2.1 (1.1-4.1)
(-)LR	0.4 (0.2-0.7)	0.3 (0.1-0.5)	0.2 (0.1-0.5)	0.7 (0.5-1.0)
AUC	0.88 (0.79-0.94)	0.92 (0.85-0.97)	0.91 (0.83-0.96)	0.72 (0.62-0.82)

Values are n (95% CI) for (+)LR and (-)LR, and n% (95% CI) for all other parameters.

AUC = area under the curve; aQFR = adenosine-flow QFR; cQFR = contrast-flow QFR; DS% = percent diameter stenosis; fQFR = fixed-flow QFR; (+)LR = positive likelihood ratio; (-)LR = negative likelihood ratio; NPV = negative predictive value; PPV = positive predictive value; QFR = quantitative flow ratio.

POTENTIAL CLINICAL APPLICATIONS OF QFR. We have demonstrated that a simple and fast computational method to derive QFR from coronary angiography without inducing pharmacologic hyperemia was feasible and accurate in determining functional lesion significance. This approach bears the potential of a wider adoption of FFR-based lesion assessment, especially in cost-constrained health care systems (where the cost of the pressure wire may be prohibitive) and in cardiac catheterization laboratories that do not offer pressure wire-based functional measurements. Similar to FFR calculated from computed tomography (10,11,29), our approach has the potential to enrich the information content of diagnostic angiography by adding functional parameters to anatomic stenosis evaluation. As such, QFR has the potential to improve diagnostic precision during invasive coronary angiography. Enhanced by accurate 3D QCA data, QFR can be used to identify culprit lesions and appropriate targets for revascularization, as well as evaluating the functional results of coronary stenting. Moreover, the computation of QFR provides both flow and pressure data, and the combination of pressure gradient and flow data.

STUDY LIMITATIONS. This study is a pilot study that compared 3 flow models. The protocol required different procedural steps, including repeated measurements for validation purposes. Given the need for repeat angiographic imaging and rewiring of target lesions, patients with severe comorbidities were not suitable candidates for inclusion and we could not investigate consecutive series of patients. The sample size is limited and we realize that an additional step is required before this method can be widely adopted, namely, a prospective comparison of core laboratory reference values with QFR obtained online in the catheterization laboratory when applied by medical and technical staff. In addition, data on clinical outcome should be obtained to assess the value of integrating this new method for the assessment of functional lesion significance into routine clinical practice. Although the current study did not show a difference in the diagnostic accuracy between cQFR and aQFR, this finding should be interpreted with caution. We cannot exclude completely that standardization and further optimization of contrast injection techniques might improve the diagnostic accuracy of cQFR and aQFR, resulting in a significant difference in accuracy between QFR computations with and without pharmacologically induced hyperemia.

In this study, only single-vessel analysis was applied. Thus, the anatomic severity of bifurcation lesions might be overestimated or underestimated, resulting in less accurate computation of pressure drop across the bifurcation. Dedicated bifurcation models (2) might improve the accuracy of QFR computation for bifurcation lesions, along with refined QCA assessment of bifurcation stenoses.

CONCLUSIONS

QFR computation improved the diagnostic accuracy of 3D QCA-based identification of stenosis significance. The favorable results of cQFR, which does not require pharmacologic hyperemia induction, but showed results similar to aQFR, bears the potential of a wide adoption of FFR-based lesion assessment through a reduction in procedure time, risk, and costs.

ACKNOWLEDGMENTS The authors acknowledge Gerhard Koning, Rolf Kooistra, Joan van't Hoog-Tuinenburg, Laurie Thomas, and Chiara De Biase for their contribution in data management and quality control. Shengxian Tu acknowledges the support by The Program for Professor of Special Appointment (Eastern Scholar) at Shanghai Institutions of Higher Learning, The Shanghai Pujiang Program (No. 15PJ1404200), and the Natural Science Foundation of China under Grant 31500797 and 81570456. Mariano Pellicano acknowledges the support by a research grant by the Cardiopath PhD program.

REPRINT REQUESTS AND CORRESPONDENCE: Dr. Shengxian Tu, Med-X Research Institute, Shanghai Jiao Tong University, No. 1954, Hua Shan Road, Shanghai 200030, China. E-mail: sxtu@sjtu.edu.cn.

PERSPECTIVES

WHAT IS KNOWN? FFR computation from coronary angiography by computational fluid dynamics offers a significant advantage over the 3D QCA-derived anatomic parameter of 50% diameter stenosis in identifying functionally significant coronary stenosis.

WHAT IS NEW? A novel and simplified approach for rapid computation of FFR, named QFR, was developed. QFR derived from coronary flow with versus without pharmacologically induced maximum hyperemia were both similarly useful to assess stenosis significance.

WHAT IS NEXT? These findings suggest that large-size outcome studies with use of QFR for clinical decision making are warranted.

REFERENCES

1. Lindstaedt M, Spiecker M, Perings C, et al. How good are experienced interventional cardiologists at predicting the functional significance of intermediate or equivocal left main coronary artery stenoses? Int J Cardiol 2007;120:254–61.

2. Tu S, Echavarria-Pinto M, von Birgelen C, et al. Fractional flow reserve and coronary bifurcation anatomy: a novel quantitative model to assess and report the stenosis severity of bifurcation lesions. J Am Coll Cardiol Cardiovasc Interv 2015;8:564–74.

3. De Bruyne B, Pijls NHJ, Kalesan B, et al. Fractional flow reserve-guided PCI versus medical therapy in stable coronary disease. N Engl J Med 2012;367:991–1001.

4. Tonino PAL, De Bruyne B, Pijls NHJ, et al. Fractional flow reserve versus angiography for guiding percutaneous coronary intervention. N Engl J Med 2009;360:213–24.

5. Johnson NP, Toth GG, Lai D, et al. Prognostic value of fractional flow reserve: linking physiologic severity to clinical outcomes. J Am Coll Cardiol 2014;64:1641–54.

6. Berry C, Corcoran D, Hennigan B, Watkins S, Layland J, Oldroyd KG. Fractional flow reserve-guided management in stable coronary disease and acute myocardial infarction: recent developments. Eur Heart J 2015;36:3155–64.

7. Fearon WF. Percutaneous coronary intervention should be guided by fractional flow reserve measurement. Circulation 2014;129:1860–70.

8. Dattilo PB, Prasad A, Honeycutt E, Wang TY, Messenger JC. Contemporary patterns of fractional flow reserve and intravascular ultrasound use among patients undergoing percutaneous coronary intervention in the united states: insights from the national cardiovascular data registry. J Am Coll Cardiol 2012;60:2337–9.

9. Toth GG, Toth B, Johnson NP, et al. Revascularization decisions in patients with stable angina and intermediate lesions: results of the international survey on interventional strategy. Circ Cardiovasc Interv 2014;7:751–9.

10. Min JK, Leipsic J, Pencina MJ, et al. Diagnostic accuracy of fractional flow reserve from anatomic CT angiography. JAMA 2012;308:1237–45.

11. Norgaard BL, Leipsic J, Gaur S, et al. Diagnostic performance of noninvasive fractional flow reserve derived from coronary computed tomography angiography in suspected coronary artery disease the NXT trial (Analysis of Coronary Blood Flow Using CT Angiography: Next Steps). J Am Coll Cardiol 2014;63:1145–55.

12. Tu S, Barbato E, Koeszegi Z, et al. Fractional flow reserve calculation from 3-dimensional quantitative coronary angiography and TIMI frame count. J Am Coll Cardiol Cardiovasc Interv 2014;7:768–77.

13. Morris PD, Ryan D, Morton AC, et al. Virtual fractional flow reserve from coronary angiography: modeling the significance of coronary lesions results from the VIRTU-1 (VIRTUal Fractional Flow Reserve From Coronary Angiography) study. J Am Coll Cardiol Cardiovasc Interv 2013;6:149–57.

14. Papafaklis MI, Muramatsu T, Ishibashi Y, et al. Fast virtual functional assessment of intermediate coronary lesions using routine angiographic data and blood flow simulation in humans: comparison with pressure wire - fractional flow reserve. EuroIntervention 2014;10:574–83.

15. Tu S, Reiber J, Li Y. Method and device for determining deviation in pressure in a blood vessel. Patent number: 60545NL. Filling date: March 18, 2014. Available at: http://www.freepatentsonline.com/y2015/0268039.html. Accessed July 6, 2016.

16. Tu S, Xu L, Ligthart J, et al. In vivo comparison of arterial lumen dimensions assessed by co-registered three-dimensional (3D) quantitative coronary angiography, intravascular ultrasound and optical coherence tomography. Int J Cardiovasc Imaging 2012;28:1315–27.

17. De Bruyne B, Paulus WJ, Pijls NH. Rationale and application of coronary transstenotic pressure gradient measurements. Cathet Cardiovasc Diagn 1994;33:250–61.

18. Kirkeeide RL. Coronary obstructions, morphology and physiologic significance. In: Reiber JHC, Serruys PW, editors. Quantitative Coronary Arteriography. Alphen aan den Rijn, Netherlands: Kluwer Academic Publishers, 1991:229–44.

19. Ofili EO, Kern MJ, St VJ, et al. Differential characterization of blood flow, velocity, and vascular resistance between proximal and distal normal epicardial human coronary arteries: analysis by intracoronary Doppler spectral flow velocity. Am Heart J 1995;130:37–46.

20. Higgins JP, Thompson SG. Quantifying heterogeneity in a meta-analysis. Stat Med 2002;21:1539–58.

21. McGee S. Simplifying likelihood ratios. J Gen Intern Med 2002;17:646–9.

22. Toth G, Hamilos M, Pyxaras S, et al. Evolving concepts of angiogram: fractional flow reserve discordances in 4000 coronary stenoses. Eur Heart J 2014;35:2831–8.

23. Johnson NP, Jeremias A, Zimmermann FM, et al. Continuum of vasodilator stress from rest to contrast medium to adenosine hyperemia for fractional flow reserve assessment. J Am Coll Cardiol Cardiovasc Interv 2016;9:757–67.

24. Leone AM, Scalone G, De Maria GL, et al. Efficacy of contrast medium induced Pd/Pa ratio in predicting functional significance of intermediate coronary artery stenosis assessed by fractional flow reserve: insights from the RINASCI study. EuroIntervention 2015;11:421–7.

25. Poon EK, Hayat U, Thondapu V, et al. Advances in three-dimensional coronary imaging and computational fluid dynamics: is virtual fractional flow reserve more than just a pretty picture? Coron Artery Dis 2015;26 Suppl 1:e43–54.

26. Li Y, Gutierrez-Chico JL, Holm NR, et al. Impact of side branch modeling on computation of endothelial shear stress in coronary artery disease: coronary tree reconstruction by fusion of 3D angiography and OCT. J Am Coll Cardiol 2015;66:125–35.

27. Tuinenburg JC, Koning G, Hekking E, et al. One core laboratory at two international sites, is that feasible? An inter-core laboratory and intra-observer variability study. Catheter Cardiovasc Interv 2002;56:333–40.

28. Gould KL, Lipscomb K, Hamilton GW. Physiologic basis for assessing critical coronary stenosis. Instantaneous flow response and regional distribution during coronary hyperemia as measures of coronary flow reserve. Am J Cardiol 1974;33:87–94.

29. Hulten E, Di Carli MF. FFR_{CT}: solid PLATFORM or thin ice? J Am Coll Cardiol 2015;66:2324–8.

KEY WORDS cardiovascular physiology, fractional flow reserve, quantitative coronary angiography

APPENDIX For a list of study investigators and expanded procedures, please see the online version of this article.